

# Development of The Zebrafish Pronephric and Mesonephric Kidneys

Cuong Q. Diep<sup>1</sup>, Noriko Mikeasky<sup>1</sup>, Alan J. Davidson<sup>2</sup>

<sup>1</sup>Department of Biology, Indiana University of Pennsylvania, Indiana, PA, United States of America; <sup>2</sup>Department of Molecular Medicine and Pathology, School of Medical Sciences, Faculty of Medical & Health Sciences, The University of Auckland, Auckland, AKL, New Zealand

## Introduction

The kidney is essential for filtering blood, expelling waste, and maintaining fluid homeostasis. These functions are performed by nephrons, which comprise tubules attached to glomeruli (blood filters) that integrate with the vasculature. Waste is excreted from the nephron into a duct system prior to leaving the body as urine. The filtrate generated at the glomerulus gets modified as it passes along different tubule segments via the reabsorption and secretion of solutes (Naylor, Qubisi, & Davidson, 2017).

Mammals form three kidney structures progressively during the embryonic development: the pronephros, mesonephros, and metanephros. The first two kidneys provide little to no renal function and degenerate, whereas the metanephros persists as the permanent adult kidney (Dressler, 2006).

In zebrafish, the pronephros is fully functional and is essential to sustain embryonic and larval life. It comprises a glomerulus and two tubules that are divided into proximal and distal segments, with each segment carrying out specific tasks that can be distinguished by the expression of specific cohorts of solute transporters. Importantly, there is considerable structural and genetic conservation between the zebrafish pronephros and mammalian nephrons, making it a useful model to study the human kidney (Naylor, Qubisi, et al., 2017).

A postembryonic metamorphosis occurs in zebrafish at around 2 weeks of age and is characterized by the gain, loss, and reorganization of many tissues (Parichy, Elizondo, Mills, Gordon, & Engeszer, 2009). The mesonephros is also formed during this phase, presumably due to increased body mass, causing a higher demand

on the renal function that cannot be met by the pronephros. This mesonephros persists as the permanent adult kidney in fish, and no metanephros is formed.

Unlike mammals, where nephrogenesis ceases around birth when kidney progenitor cells become exhausted, nephrogenesis in zebrafish is continuous throughout the adult life (Zhou, Boucher, Bollig, Englert, & Hildebrandt, 2010). As fish grow, their kidneys also increase in size by the addition of new nephrons. In response to kidney injury from nephrotoxins, such as gentamicin, the rate of de novo mesonephrogenesis increases as part of a regenerative response. In addition, the damaged nephrons are also capable of undergoing self-repair, a process that appears similar to mammalian nephron repair (Johnson, Holzemer, & Wingert, 2011). With features that are unique and in common with the mammalian kidney, the zebrafish kidney serves as an alternative model for understanding kidney development, disease, and repair (Jerman & Sun, 2017).

## Structure of The Pronephros and Mesonephros

The pronephros comes from the mesoderm germ layer that is created during gastrulation. The mesoderm becomes divided into the paraxial mesoderm, lateral plate mesoderm, and intermediate mesoderm (IM). The IM, located between the other mesoderm layers, is the source of the pronephros. At the end of gastrulation, the IM appears as bilateral stripes on either side of the embryonic trunk and proliferates during early somitogenesis stages (10–16 h post fertilization; hpf) in response to Wnt8a, a member of the Wnt family of secreted factors. This early wave of growth expands

the pool of pronephric progenitors prior to their differentiation into renal epithelial cells (Naylor, Han, Hukriede, & Davidson, 2017).

At around 48 hpf, the pronephros becomes functional (albeit not yet fully mature) and comprises bilateral nephrons with fused glomeruli in the anterior trunk and tubules that run to the cloaca at the posterior. The glomeruli (G) are connected to the tubules via a short neck segment containing motile cilia. The tubules are divided into four functionally distinct segments: proximal convoluted tubule (PCT), proximal straight tubule (PST), distal early tubule (DE), and distal late tubule (DL) (Fig. 15.1). Recent data suggest that the DL segment serves a dual tubule/duct function (Naylor, Qubisi, et al., 2017) and while the posterior terminus of the DL segment has been considered to be solely ductal in nature (Wingert et al., 2007), further work is needed to clarify the identity of this region.

The pronephros likely gets overwhelmed in larger juveniles with a higher body mass. For coping with this, the mesonephros is formed by the addition of new nephrons onto the existing pronephros. Mesonephrogenesis during this larva-to-juvenile transition occurs during metamorphosis at around 14 days post fertilization (dpf) (Diep et al., 2011; Zhou et al., 2010). The first mesonephric nephron appears at the ~5.2 mm total length stage (13–14 dpf), based on detection of *cdh17* and *podocin* transcripts. It is located at the level of the sixth somite on top of the distal portion of the pronephric DE segment (Fig. 15.2A). The second and third mesonephric nephrons form level with the seventh and eighth somites, respectively. This stereotypical pattern is short-lived, and from the 6.5 mm stage onwards nephrons appear randomly near the most proximal portion of the DE segment in the position of the future head kidney and on top of both the DE and DL segments (Fig. 15.2B). By 9 mm, the nascent mesonephros morphologically resembles the adult kidney and has the head, trunk, and tail regions (Fig. 15.3) (Diep et al., 2011, 2015; Zhou et al., 2010). Successive waves of nephrogenesis result in a complex network of interconnected

nephrons that plumb into pronephric and mesonephric DE and DL segments. It is hypothesized that the pronephric DE and DL segments eventually transform into the two major collecting ducts that run down the midline of the adult mesonephros (Fig. 15.2C) (Diep et al., 2015).

## Formation of The Pronephros

Early pronephric progenitors can be subdivided into rostral and caudal populations based on the expression of Notch receptor ligands (*deltaC* and *jagged2a*) and the *mecom* transcription factor gene, respectively (Li, Cheng, Verdun, & Wingert, 2014). The rostral domain corresponds to podocyte, neck, PCT, PST, and DE progenitors, while the caudal domain corresponds to DL progenitors (Naylor, Dodd, & Davidson, 2016). The relative sizes of the rostral and caudal domains are established by retinoic acid (RA) signaling during gastrulation and early somitogenesis stages (Naylor, Skvarca, et al., 2016; Wingert et al., 2007). RA signaling promotes rostral gene expression but is believed to be degraded in more caudal portions of the IM by the *Cyp26a1* enzyme (Naylor, Skvarca, et al., 2016; Wingert et al., 2007).

The effect of RA likely occurs through the expression of downstream transcription factors. In the most anterior IM (but also in the surrounding mesoderm), RA appears to directly induce the expression of the *Wilms' tumor suppressor-1a* (*wt1a*) transcription factor gene. *Wt1a* plays a central role in directing IM cells to differentiate into podocytes, which are key filtration cells in the glomerulus (Tomar, Mudumana, Pathak, Hukriede, & Drummond, 2014). The Notch ligands *jagged1b* and *jagged2b* are also dependent on RA signaling for their early expression in the anterior IM and have been implicated in podocyte formation (O'Brien et al., 2011).

The partially redundant transcription factor genes *pax2a* and *pax8* are the earliest markers of the IM and are expressed along its entire length, without

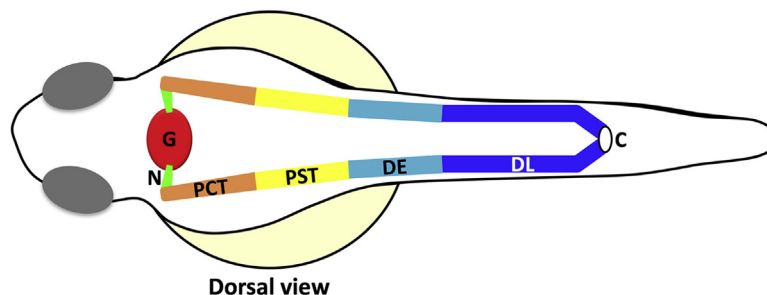


**FIGURE 15.1 Pronephros structure.** The pronephros at 48 hpf comprises a central fused glomerulus, and this is connected to the bilateral tubules by short neck segments. The tubule is divided into four functionally distinct segments that express specific solute transporters. (G, glomerulus; N, neck segment; PCT, proximal convoluted tubule; PST, proximal straight tubule; DE, distal early tubule; DL, distal late tubule; C, cloaca).

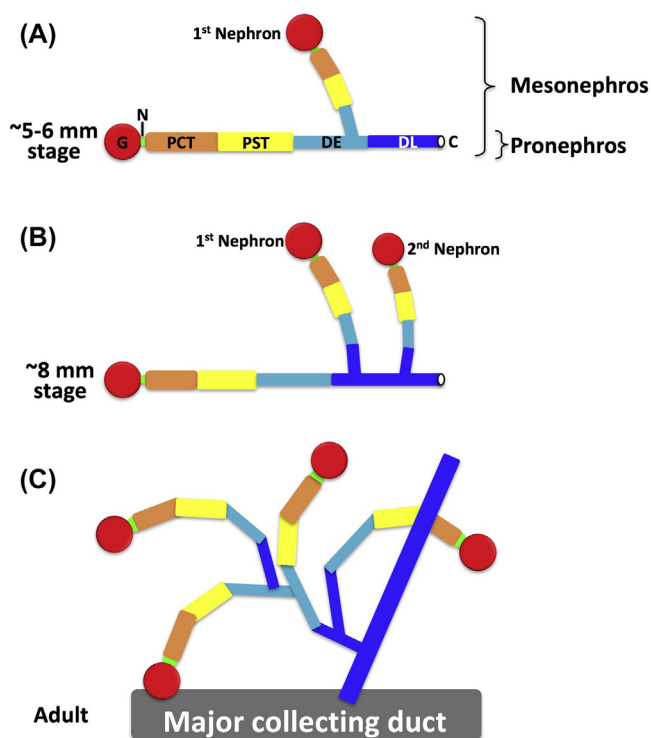


**FIGURE 15.2 Mesonephros structure.** (A) The first mesonephric nephron appears in  $\sim 5.2$  mm larvae at the distal portion of the pronephric DE segment. (B) At the  $\sim 8$  mm stage, more mesonephric nephrons are present on top of the pronephric DE (not shown) and DL segments. (C) The adult mesonephros has an interconnected network of nephrons, where branching occurs at the DE and DL segments and waste is drained into the bilateral major collecting ducts.

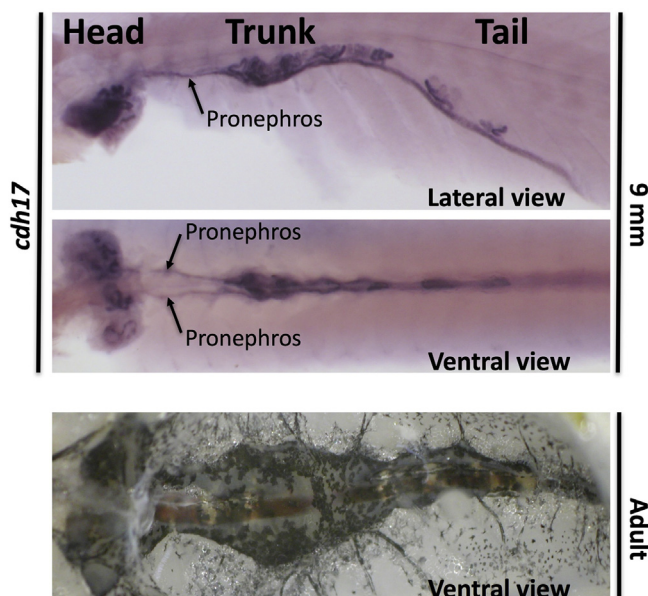


**FIGURE 15.3 Mesonephros morphology.** The nascent mesonephros at 9 mm morphologically resembles the adult mesonephros, where both consist of a head, trunk, and tail region. The pronephros (bilateral tubules running the length of the trunk) serves as a scaffold for the addition of mesonephric nephrons. The top and middle images (of the same animal) are from in-situ hybridization with probes for *cdh17*. The bottom image is of an adult kidney inside the body cavity.

dependency on RA signaling. Double knockdown of *pax2a* and *pax8* has revealed their requirement for tubule differentiation and as likely upstream inducers of the *hnf1ba/b* paralogs (herein referred to as *hnf1b*) encoding homeobox-containing transcription factors (Naylor, Przepiorski, Ren, Yu, & Davidson, 2013). *Hnf1b* is essential for pronephric tubule maturation into the four segments and the activation of segment-specific marker genes, such as the solute transporter genes *slc20a1a* (PCT), *trpm7* (PST), *slc12a1* (DE), and *slc12a3* (DL) (Naylor et al., 2013) (Fig. 15.1). How different segment identities are induced downstream of the  $Pax2/8 \rightarrow Hnf1b$  pathway remains uncertain but additional transcription factors, such as *Sim1* (PST), *Irx3b* (DE), and *Mecom* (DL) may contribute to specific segmental fates and/or their proliferation (Cheng & Wingert, 2015; Li et al., 2014; Wingert & Davidson, 2011).

There is also an intrasegmental diversification in cell phenotype with some cells in the PCT, PST, and DE segments developing bundles of motile cilia that aid in the movement of the filtrate along the pronephros to the cloaca. These multiciliated cells are present in a “salt and pepper” pattern and are thought to be regulated by the Notch pathway, via a classic lateral inhibition mechanism, and the *Etv4/Etv5a* transcription factors (Marra & Wingert, 2016).

During tubulogenesis, the IM undergoes a mesenchymal-to-epithelial transition beginning around the 12–14 somite stage ( $\sim 14$  hpf) and forms a lumenized tubule by the 20 somite stage (21 hpf). There is also evidence for tight junctions between the tubular epithelial cells. Based on the expression of *claudin* genes (encoding components of the tight junction that control the paracellular flow of molecules) it can be inferred that the PCT and PST segments are more “leaky” than the DE and DL segments, similar to what is found in the mammalian nephron (McKee, Gerlach, Jou, Cheng, & Wingert, 2014; Naylor & Davidson, 2014).

The tubule cells also contain adherens junctions that maintain cell-to-cell adhesion via homotypic interactions between cadherins. The cadherin genes of importance in the zebrafish pronephros include *cadherin-17*, which is expressed in all tubule segments and its knockdown results in a general loss in tubule cell adhesion (Horsfield et al., 2002), *cadherin-6* in podocyte and neck precursors (Kubota, Murakami, Mogi, & Yorifuji, 2007), and *cadherin-1* (E-cadherin) in the DL segment (Naylor et al., 2013).

Around the time that tubule epithelialization is occurring (12–20 somite stage), and cells become adhered to one another, the tubular cells also undergo dynamic morphological changes. Current evidence indicates that the DL segment compacts as it migrates and fuses with the cloaca, leading to a pulling and stretching of the PST and DE segments (Naylor, Dodd, et al., 2016). Thus, as tubulogenesis proceeds, the rostral domain



(comprising PCT, PST, and DE progenitors) becomes progressively elongated while the caudal domain (DL progenitors) shortens. The tension applied to the DE segment, and possibly also the PST segment, during this process is believed to drive stretch-induced proliferation and contribute to a second (post-Wnt8a) wave of tubule growth (Naylor, Han, et al., 2017).

Starting around the 18 somite stage and progressing to 48 hpf, the podocyte precursors migrate to the midline, fuse, and recruit a blood supply from the overlying dorsal aorta (Drummond et al., 1998). While filtration starts around this time, the glomerular filter is not fully mature until 96 hpf when it shows size-selectivity and fully differentiated podocytes (Kramer-Zucker, Wiessner, Jensen, & Drummond, 2005).

Once flow initiates in the tubule, a collective cell migration process initiates in the PCT, resulting in its compaction and convolution (Vasilyev et al., 2009). The proximal compaction here exerts a new mechanical tension on the tubule but this time in the opposite direction to that seen at the earlier stage. This leads to the stretching and elongation of the more distal segments (particularly the DE) and stretch-induced proliferation (comprising the third wave of tubule growth) (Naylor, Dodd, et al., 2016). As a result, the DE segment increases significantly in length until the 5 mm stage at which point it reaches its maximal length and extends over the swim bladder just caudal of the glomerulus (Diep et al., 2015).

### Formation of The Mesonephros

Mesonephrogenesis is initiated when a few single mesenchymal progenitor cells coalesce into a basophilic cluster. The progenitors are labeled in the *Tg(lhx1a:EGFP)* transgenic line. Single *lhx1a:EGFP*<sup>+</sup> cells are seen attached to the top of the pronephric DE segment at the ~4 mm (~10 dpf) stage. More progenitors appear later along the length of the pronephric tubules together with *lhx1a:EGFP*<sup>+</sup> clusters. Single progenitors have filopodia-like projections that may be involved in their migration toward each other and to distant sites of nephrogenesis.

*lhx1a:EGFP*<sup>+</sup> clusters express nephron progenitor markers (*wt1b*, *pax2a*, *lhx1a*) and proliferate. They epithelialize into “renal vesicles” and then elongate into nascent nephrons with restricted marker gene expression. For instance, transcripts for *wt1b* (a paralog of *wt1a*) are detected in the future glomerulus while *lhx1a* and *pax8* are expressed in more distal nephron regions. In the mammalian metanephros, Wnt9b induces nephrogenesis (Carroll, Park, Hayashi, Majumdar, &

McMahon, 2005) and it is interesting to note that *wnt9a* is expressed in the pronephric distal tubules after 4 dpf, making it a potential nephron-inducing candidate (Curtin, Hickey, Kamel, Davidson, & Liao, 2011). Indeed, recent findings show that *wnt9a/b* are expressed in the distal tubules and collecting ducts during regeneration and that the canonical Wnt signaling pathway regulates the proliferation of nephron progenitor cells and morphogenesis of nascent nephrons (Kamei, Gallegos, Liu, Hukriede, & Drummond, 2019). Further research is needed to determine whether similar events occur during mesonephros development.

The first mesonephric nephron becomes functional at the ~6 mm stage and initially comprises a nephron with a glomerulus-neck-PCT-PST-DE structure. It becomes fused to the pronephric DE segment, resulting in a DE-to-DE junction (Fig. 15.2A). However, at later stages, this nascent mesonephric nephron acquires a DL segment that expresses *slc12a3*, and a DL-to-DL junction is seen with the pronephros (Fig. 15.2B). Whether this phenomenon is the result of transdifferentiation events occurring in these mesonephric and pronephric segments is unclear and requires more investigation.

By the ~8 mm stage, numerous mesonephric nephrons are formed with their DL segments fusing to the pronephric DL segment, and thus, draining into a common pronephric tubule (Fig. 15.2B). Eventually, the pronephric glomerulus is lost, supporting the idea that the pronephros eventually loses kidney function to become a scaffold for the mesonephros. In this hypothesis, the bilateral pronephric tubules become the two major collecting ducts where all the mesonephric nephrons drain their waste. The first wave of mesonephrogenesis provides primary nephrons that fuse directly onto the pronephric DE and DL segments (Fig. 15.2B). Later waves of nephrogenesis produce nephrons that fuse onto primary nephrons, resulting in branching predominantly at the DL segment, as revealed by the expression of the *slc12a3* (DL) in adult kidneys, but in some cases, fusion also occurs with the DE segment (Diep et al., 2011). Overall, common genes (*lhx1a*, *pax2a*, *wt1b*) are associated with the development of both pronephros and mesonephros, and the nephrons in both kidneys share a conserved segmentation pattern (Figs. 15.1 and 15.2).

Mesonephrogenesis continues during juvenile life at a linear rate with respect to body mass or length (Diep et al., 2011; Zhou et al., 2010). In adults, nephrogenesis is decreased to a basal rate with approximately two renal vesicles (*lhx1a*<sup>+</sup>, *wt1b*<sup>+</sup>) in a normal kidney at any one time, and there are approximately 300 total nephrons

in the mesonephros of 1-year old fish (Diep et al., 2011; Zhou et al., 2010).

The rate of nephrogenesis is increased in response to acute kidney injury, such as that induced by intraperitoneal injection of the nephrotoxin gentamicin. Within 8 h, all nephrons lose expression of the PCT marker *slc20a1a* and cannot absorb filtered dextran. Around 4–6 days later, some damaged nephrons reexpress *slc20a1a* and begin reabsorbing dextran again, consistent with the damaged nephrons undergoing self-repair, a feature shared with mammals (Diep et al., 2011). Notable at this time is the appearance of numerous nascent nephrons. These new nephrons are presumed to have arisen from basophilic clusters that were either pre-existing, perhaps in a “poised” state, or induced to form from single nephron progenitors. By four to 6 weeks after injury, the kidney is largely repaired and repopulated with nephrons. These are assumed to be a mix of repaired nephrons and newly generated nephrons. However, it is challenging to assess the proportion of nephrons that have repaired from those arising de novo.

New nephrons successfully integrate with the vasculature and the existing tubule/collecting duct network. They are capable of absorbing filtered dextran, and histological sections confirm that new basophilic tubules fuse with mature existing nephrons to share a common lumen (Fig. 15.4). The fusion of new nephrons to an existing kidney architecture is an essential process when considering future cell-based therapies that seek to replace nephrons in damaged human kidneys. In this respect, larval mesonephrogenesis may be a

good model for furthering our understanding of the steps involved.

## Concluding Remarks

The zebrafish has been an important model for understanding kidney development, regeneration, and disease. The pronephros is simple with two mostly linear nephrons, making it ideal for studying the developmental processes that govern kidney formation such as specification from mesoderm, progenitor proliferation, the transcription factor networks that drive differentiation, and the morphological changes, such as collective cell migration and compaction that influence the final form and function of the kidney. The mesonephros is emerging as an attractive model for understanding how transplanted nephron progenitors can migrate and self-organize into nephrons, and how new nephrons integrate into an existing kidney—processes that are at the heart of future regenerative therapies in humans.

## References

- Carroll, T. J., Park, J. S., Hayashi, S., Majumdar, A., & McMahon, A. P. (2005). Wnt9b plays a central role in the regulation of mesenchymal to epithelial transitions underlying organogenesis of the mammalian urogenital system. *Developmental Cell*, 9(2), 283–292.
- Cheng, C. N., & Wingert, R. A. (2015). Nephron proximal tubule patterning and corpuscles of Stannius formation are regulated by the *sim1a* transcription factor and retinoic acid in zebrafish. *Developmental Biology*, 399(1), 100–116.
- Curtin, E., Hickey, G., Kamel, G., Davidson, A. J., & Liao, E. C. (2011). Zebrafish *wnt9a* is expressed in pharyngeal ectoderm and is required for palate and lower jaw development. *Mechanisms of Development*, 128(1–2), 104–115.
- Diep, C. Q., Ma, D., Deo, R. C., Holm, T. M., Naylor, R. W., Arora, N., et al. (2011). Identification of adult nephron progenitors capable of kidney regeneration in zebrafish. *Nature*, 470(7332), 95–100.
- Diep, C. Q., Ukah, T. K., Kelly, P. M., Peng, Z., Daigle, R. V., & Davidson, A. J. (2015). Development of the zebrafish mesonephros. *Genesis*, 53(3–4), 257–269.
- Dressler, G. R. (2006). The cellular basis of kidney development. *Annual Review of Cell and Developmental Biology*, 22, 509–529.
- Drummond, I. A., Majumdar, A., Hentschel, H., Elger, M., Solnica-Krezel, L., Schier, A. F., et al. (1998). Early development of the zebrafish pronephros and analysis of mutations affecting pronephric function. *Development*, 125(23), 4655–4667.
- Horsfield, J., Ramachandran, A., Reuter, K., LaVallie, E., Collins-Racie, L., Crosier, K., et al. (2002). Cadherin-17 is required to maintain pronephric duct integrity during zebrafish development. *Mechanisms of Development*, 115(1–2), 15–26.
- Jerman, S., & Sun, Z. (2017). Using zebrafish to study kidney development and disease. *Current Topics in Developmental Biology*, 124, 41–79.

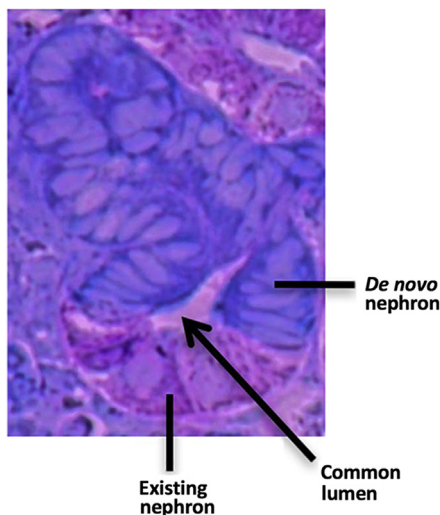


**FIGURE 15.4** Integration of new and existing nephrons. De novo nephrons fuse with existing nephrons to share a common lumen.

- Johnson, C. S., Holzemer, N. F., & Wingert, R. A. (2011). Laser ablation of the zebrafish pronephros to study renal epithelial regeneration. *Journal of Visualized Experiments : Journal of Visualized Experiments*, (54).
- Kamei, C. N., Gallegos, T. F., Liu, Y., Hukriede, N., & Drummond, I. A. (2019). Wnt signaling mediates new nephron formation during zebrafish kidney regeneration. *Development*, 146(8). <https://doi.org/10.1242/dev.168294>.
- Kramer-Zucker, A. G., Wiessner, S., Jensen, A. M., & Drummond, I. A. (2005). Organization of the pronephric filtration apparatus in zebrafish requires Nephhrin, Podocin and the FERM domain protein Mosaic eyes. *Developmental Biology*, 285(2), 316–329.
- Kubota, F., Murakami, T., Mogi, K., & Yorifuji, H. (2007). Cadherin-6 is required for zebrafish nephrogenesis during early development. *International Journal of Developmental Biology*, 51(2), 123–129.
- Li, Y., Cheng, C. N., Verdun, V. A., & Wingert, R. A. (2014). Zebrafish nephrogenesis is regulated by interactions between retinoic acid, mecom, and Notch signaling. *Developmental Biology*, 386(1), 111–122.
- Marra, A. N., & Wingert, R. A. (2016). Epithelial cell fate in the nephron tubule is mediated by the ETS transcription factors *etv5a* and *etv4* during zebrafish kidney development. *Developmental Biology*, 411(2), 231–245.
- McKee, R., Gerlach, G. F., Jou, J., Cheng, C. N., & Wingert, R. A. (2014). Temporal and spatial expression of tight junction genes during zebrafish pronephros development. *Gene Expression Patterns: GEP*, 16(2), 104–113.
- Naylor, R. W., & Davidson, A. J. (2014). *Hnf1beta* and nephron segmentation. *Pediatric Nephrology*, 29(4), 659–664.
- Naylor, R. W., Dodd, R. C., & Davidson, A. J. (2016). Caudal migration and proliferation of renal progenitors regulates early nephron segment size in zebrafish. *Scientific Reports*, 6, 35647.
- Naylor, R. W., Han, H. I., Hukriede, N. A., & Davidson, A. J. (2017). *Wnt8a* expands the pool of embryonic kidney progenitors in zebrafish. *Developmental Biology*, 425(2), 130–141.
- Naylor, R. W., Przepiorski, A., Ren, Q., Yu, J., & Davidson, A. J. (2013). *HNF1beta* is essential for nephron segmentation during nephrogenesis. *Journal of the American Society of Nephrology: Journal of the American Society of Nephrology*, 24(1), 77–87.
- Naylor, R. W., Qubisi, S. S., & Davidson, A. J. (2017). Zebrafish pronephros development. *Results and Problems in Cell Differentiation*, 60, 27–53.
- Naylor, R. W., Skvarca, L. B., Thisse, C., Thisse, B., Hukriede, N. A., & Davidson, A. J. (2016). BMP and retinoic acid regulate anterior-posterior patterning of the non-axial mesoderm across the dorsal-ventral axis. *Nature Communications*, 7, 12197.
- O'Brien, L. L., Grimaldi, M., Kostun, Z., Wingert, R. A., Selleck, R., & Davidson, A. J. (2011). *Wt1a*, *Foxc1a*, and the notch mediator *Rbpj* physically interact and regulate the formation of podocytes in zebrafish. *Developmental Biology*, 358(2), 318–330.
- Parichy, D., Elizondo, M., Mills, M., Gordon, T., & Engeszer, R. (2009). Normal table of postembryonic zebrafish development: Staging by externally visible anatomy of the living fish. *Developmental Dynamics : An Official Publication of the American Association of Anatomists*, 238(12), 2975–3015.
- Tomar, R., Mudumana, S. P., Pathak, N., Hukriede, N. A., & Drummond, I. A. (2014). *osr1* is required for podocyte development downstream of *wt1a*. *Journal of the American Society of Nephrology: Journal of the American Society of Nephrology*, 25(11), 2539–2545.
- Vasilyev, A., Liu, Y., Mudumana, S., Mangos, S., Lam, P. Y., Majumdar, A., et al. (2009). Collective cell migration drives morphogenesis of the kidney nephron. *PLoS Biology*, 7(1), e9.
- Wingert, R. A., & Davidson, A. J. (2011). Zebrafish nephrogenesis involves dynamic spatiotemporal expression changes in renal progenitors and essential signals from retinoic acid and *irx3b*. *Developmental Dynamics : An Official Publication of the American Association of Anatomists*, 240(8), 2011–2027.
- Wingert, R. A., Selleck, R., Yu, J., Song, H. D., Chen, Z., Song, A., et al. (2007). The *cdx* genes and retinoic acid control the positioning and segmentation of the zebrafish pronephros. *PLoS Genetics*, 3(10), 1922–1938.
- Zhou, W., Boucher, R. C., Bollig, F., Englert, C., & Hildebrandt, F. (2010). Characterization of mesonephric development and regeneration using transgenic zebrafish. *American Journal of Physiology. Renal Physiology*, 299(5), F1040–F1047.